



Porosity sensitivity of A356 Al alloy during fiber laser welding

Kai LI^{1,2}, Feng-gui LU^{1,2}, Song-tao GUO¹, Hai-chao CUI^{1,2}, Xin-hua TANG^{1,2}

1. School of Materials Science and Engineering, Shanghai Jiao Tong University, Shanghai 200240, China;

2. Shanghai Key Laboratory of Materials Laser Processing and Modification,
Shanghai Jiao Tong University, Shanghai 200240, China

Received 13 October 2014; accepted 7 May 2015

Abstract: In order to decrease the metallurgical porosity and keyhole-induced porosity during deep penetration laser welding of Al and its alloys, and increase the mechanical properties of work-piece, the effects of welding parameters such as laser power, welding speed and defocusing value on both kinds of porosities were systemically analyzed respectively, and the shape and fluctuation of plume of the keyhole were observed to reflect the stability of the keyhole. The results show that increasing laser power or decreasing laser spot size can lead to the rising of both number and occupied area of pores in the weld; meanwhile, the plume fluctuates violently over the keyhole, which is always accompanied with the intense metallic vapor, liquid metal spatter and collapsing in the keyhole, thus more pores are generated in the weld. The porosity in the weld reaches the minimum at welding velocity of 2.0 m/min when laser power is 5 kW and defocusing value is 0.

Key words: A356 Al alloy; fiber laser welding; porosity; keyhole; plume

1 Introduction

As one of the most advanced technologies, laser welding has gotten a huge development in recent decades, which makes it possible to realize a high quality weld on Al thick plate [1,2]. However, porosity, as one of most serious defects in the weld, which would affect the mechanical property of weld structure negatively, can be easily induced in deep penetration laser welding on Al and its alloys.

Two different types of porosities (metallurgical porosity and keyhole-induced porosity) may form during keyhole laser welding [3]. As the most common type of porosity, the formation of metallurgical porosity mainly depends on the metallurgical reaction and solubility variation of gas in liquid metal during welding. When the temperature of liquid aluminum decreases from over 1200 to 930 K at solidus point, the solubility of H in aluminum reduces dramatically [4]. The great difference in solubility makes H₂ evolved from molten pool, and the bubbles with H₂ inside are then captured by moving solidification interface and result in porosity finally. Besides, some bubbles can float out of the molten pool

before the solidification interface arrives. CO and N₂ are also common gases detected in metallurgical porosity [5]. Different from metallurgical porosity, keyhole-induced porosity occurs only when the stability of keyhole is undermined in keyhole laser welding. The gas in porosity is mainly the shielding gas (Ar or He, etc.), which is isolated by molten pool.

Many researchers have studied the formation mechanism and prevention methods of keyhole-induced porosity in recent years. KATAYAMA et al [6] studied the keyhole formation process with a high speed X-radiography, and found that the front wall of molten pool exposed to laser beam caused amounts of metal vapor strongly impacting on the rear wall of molten pool, and then induced bubbles and pores. KAWAGUCHI et al [7] analyzed the pores induced by the stability of slender liquid column, and found that the number of pores in weld grew with the increase of depth-to-width ratio. SETO et al [8] found that the variation of plasma induced in welding process had some relationship with the stability of keyhole, and the plasma was affected by several factors, such as different shielding gases and metals. YAO and GONG [3] adopted a dual laser beam system to enlarge the opening of keyhole, and improved

the fluctuating conditions of the keyhole wall and decreased the amount of keyhole-induced porosity. NORRIS et al [9] found that more pores can be generated at the root of keyhole easily at lower welding velocity and higher laser power, and the average diameter of porosity got larger when heat input and spot size increased. Also, many other parameters were studied, such as the replacement of continuous laser wave by pulsed laser wave [10–12] and the adoption of laser-MIG hybrid welding [13]. On the other hand, many numerical modeling researches about keyhole laser welding have been done in recent years to study the physical mechanism and formation process of keyhole [14–19]. However, although keyhole-induced porosity and metallurgical porosity have been fully studied respectively, researches on method to control both of them are still relatively little. Since these two kinds of porosities are familiar during keyhole laser welding on aluminum and its alloy, it is essential to distinguish them, and then reduce the number and area of the porosities, especially the keyhole-induced porosity, for its irregular shape can do much more harm to the mechanical property of welded joint.

A new method to distinguish the type of porosity was studied in this work, and the numbers and occupied areas of both metallurgical porosity and keyhole-induced porosity were calculated respectively in the experiment under different process parameters. Also, the photos of plume and spatter in welding process were captured with 1000 fps (frame per second) high-speed camera to analyze the stability of keyhole under different welding parameters.

2 Experimental

The schematic diagram of fiber laser welding on 8 mm-thick plate of A356 Al alloy is shown in Fig. 1, where an ytterbium laser system–10000 with a maximum output power of 10 kW was used to weld the Al alloy plate. High-speed camera with 1000 fps was introduced to systematically investigate the behavior of plume induced during the welding process. 99.95% argon was used as shielding gas to keep the molten pool from being oxidized, the blowing flow rate of argon was adjusted to

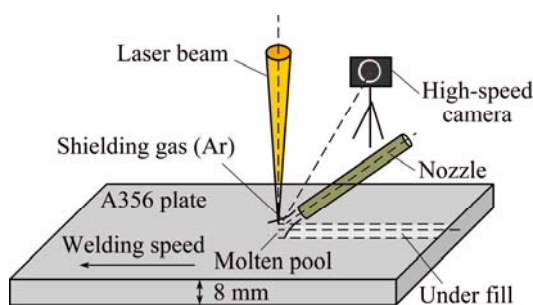


Fig. 1 Schematic diagram of laser welding on A356 Al plate

15 L/min, and argon gas blew the same direction with welding velocity. The chemical component of A356 Al alloy is shown in Table 1.

Table 1 Chemical composition of A356 Al alloy used in experiment (mass fraction, %)

Si	Mg	Ti	Fe	Cu
7.39	0.37	0.15	≤0.16	≤0.05
Mn	Zn	Sn	Pb	Al
≤0.10	≤0.05	≤0.01	≤0.03	Bal.

The plate surface was polished by steel brush before the welding process, and then rinsed with pure alcohol to remove the dirt and moisture. After welding, a specimen with dimensions of 60 mm (length) × 30 mm (width) × 8 mm (height) was obtained from the weld, 20 mm away from the starting point of welding, then cut into two pieces along the weld center, and corroded by Keller's reagent (1 mL HF, 2.5 mL HNO₃, 1.5 mL HCl and 95 mL H₂O) for calculating the occupied area percentage μ and number of pores ($d > 1.0$ mm), which can be expressed as follows:

$$\mu = \frac{\sum S_i}{S} \quad (1)$$

where S_i represents the occupied cross-section area of each type of porosity on the longitude section of weld bead, and S stands for the occupied area of weld bead on the section.

After corrosion, the coupon was photographed by a stereomicroscope (Stem 2000) to count S_i and S . The microstructures of the inner wall surface of pores were then observed with a FESEM (field emission scanning electron microscope, JSM 7600F), to distinguish the difference between keyhole-induced porosity and metallurgical porosity.

3 Result and discussion

3.1 Morphologies of different porosities

When the forces (surface tension, recoil pressure, hydrodynamic pressure and hydrostatic pressure) on the keyhole are out of balance, the keyhole turns unstable and collapse happens during welding process, so shielding gas inside the keyhole gets isolated due to the collapse, the gases in molten pool develop to bubbles, and bubble which is adjacent to keyhole root can be easily captured by solidification interface at the bottom of molten pool, then transforms into porosity. Meanwhile, gases like H₂ dissolve out from the molten pool because of the solubility change during the solidification process, the bubbles with H₂ inside are usually formed at random locations in the molten pool, and could be captured when

they float to the surface of molten pool. The difference of formation mechanism for these two kinds of porosities results in the variation of distribution location and appearance of them.

The distribution of porosity on the longitudinal section of the weld is shown in Fig. 2(a). Pores with irregular profile are found mostly at the root of the weld near the fusion line, while pores with smooth surface and sphere shape are usually found at the middle of the weld. The shape of keyhole is irregular, thus the isolated part with shielding gas inside is random-shaped, too. For the other one, the formation process of metallurgical porosity includes four parts: 1) gases like H_2 dissolve

from molten pool to form small bubbles; 2) small bubbles gather into big bubbles while floating up to the surface of molten pool; 3) big bubbles float up; 4) bubbles get captured by moving solidification interface while floating and form metallurgical porosity. The surface tension on bubbles which went through a process of floating up has enough time to make the bubble a sphere shape. Thus, it can be inferred that porosity with regular shape and smooth surface should be metallurgical porosity and the others are keyhole-induced pores.

Figures 2(b) and (c) exhibit the morphologies of metallurgical porosity and keyhole-induced porosity, respectively. Metallurgical porosity with a sphere shape

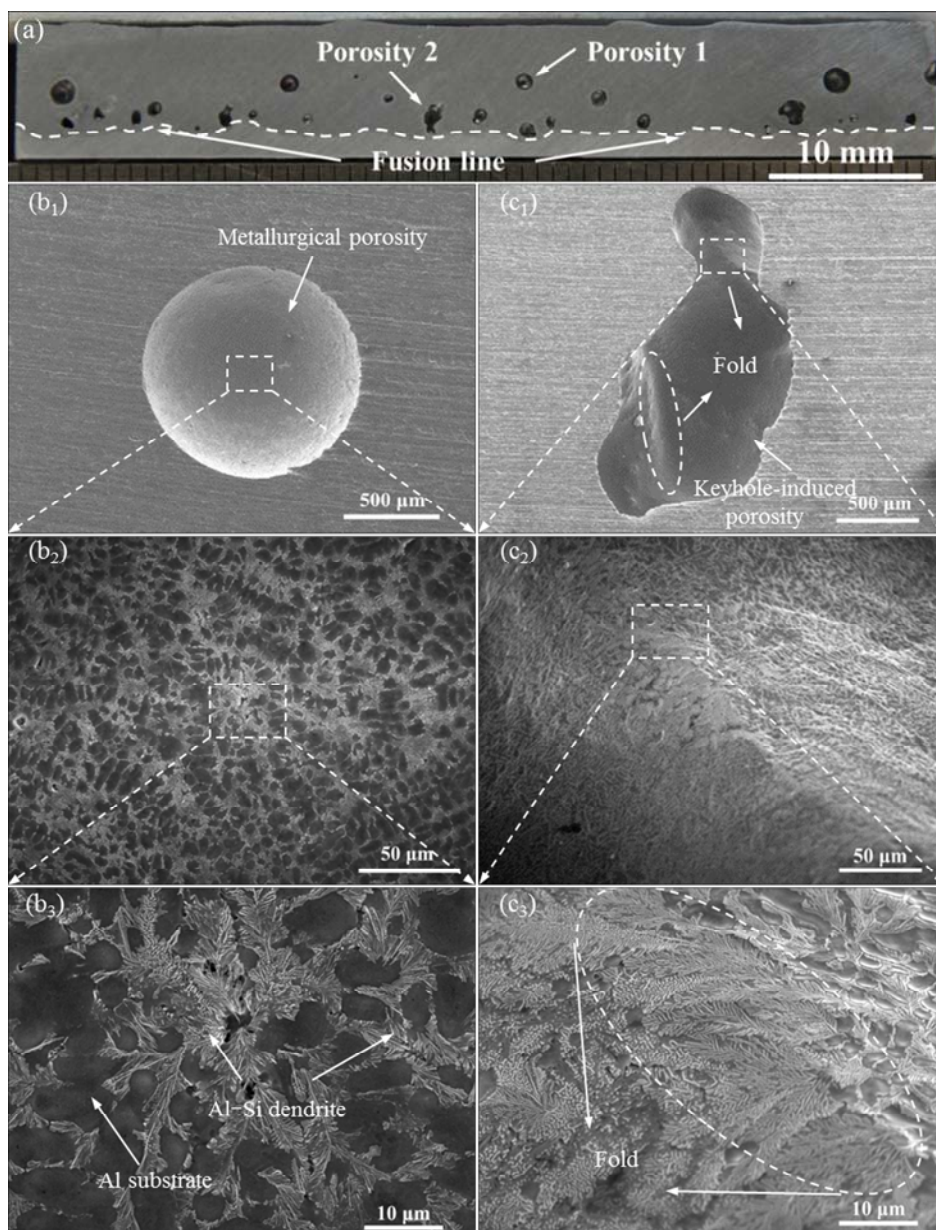


Fig. 2 Morphologies of metallurgical and keyhole-induced porosities: (a) Distribution of porosity on longitudinal section of weld; (b₁) Full view of metallurgical porosity; (b₂, b₃) Details with enlarged scale inside metallurgical porosity; (c₁) Full view of keyhole-induced porosity; (c₂, c₃) Details with enlarged scale inside keyhole-induced porosity (fold can be obviously seen inside irregular porosity, and shape and size of Al-Si grain differ from each other on two sides of fold)

and smooth surface is shown in Fig. 2(b₁), the diameter of the porosity is around 1.1 mm, and detailed characterization inside porosity is shown in Fig. 2(b₂), where the microstructures distribute uniformly and typical Al–Si dendrite can be observed on the inner wall of metallurgical porosity. Because of the sphere shape, the temperature gradient is evenly distributed on the inner wall of keyhole, so the microstructures are distributed orderly as observed. However, for keyhole-induced porosity, the temperature gradient which can determine the growth of grain is much more complex on the inner wall due to the irregular shape of porosity, which leads to different sizes of grain and non-uniform distribution of Al–Si dendrite. Figure 2(c₁) displays the appearance of keyhole-induced porosity, the shape of porosity is irregular and some convexity locations (called as fold) occur inside the porosity. Rough surface can be obviously observed and Al–Si microstructures are distributed non-uniformly, as shown in Figs. 2(c₂) and (c₃).

3.2 Effect of process parameters on porosity

To identify how different factors affect the keyhole stability and the two kinds of porosities in the weld, process parameters such as laser power (P), welding velocity (v_w) and defocusing value (D) were studied in this work, as shown in Table 2. Laser power varies from 3 to 5 kW, welding velocity varies from 1 to 2.5 m/min, and defocusing value distributes from 0 to +15 mm.

Table 2 Different process parameters in experiment

Test No.	Laser power/ kW	Welding velocity/ (m·min ⁻¹)	Defocusing value/mm
1	5.0	1.0	0
2	4.5	1.0	0
3	4.0	1.0	0
4	3.5	1.0	0
5	3.0	1.0	0
6	5.0	1.5	0
7	5.0	2.0	0
8	5.0	2.5	0
9	5.0	1.0	+5
10	5.0	1.0	+10
11	5.0	1.0	+15

Figure 3 shows the porosity area percentage μ on the longitudinal section of weld and the number of large porosity ($d > 1.0$ mm). The porosity has an area more than 0.79 mm^2 , which is corresponding to the occupied area of a spherical porosity with a diameter of 1 mm (about 0.79 mm^2).

As shown in Figs. 3(a) and (b), with increasing the laser power, both the porosity area percentage and

number of porosity ($d > 1.0$ mm) get larger, especially for the number of porosity. The recoil pressure on the keyhole gets higher and the impact of metallic vapor inside keyhole becomes more intense as the heat input and energy density rose, which lead to the unbalance of forces in keyhole, causing the instability and multi-collapse in keyhole. Therefore, more bubbles generated at the root of keyhole and more porosity remained in weld as a result.

Figures 3(c) and (d) reveal that the area percentage of metallurgical porosity decreases to lower than 1.0% when welding velocity is higher than 1.5 m/min, while it is 2.2% at 1.0 m/min. For keyhole-induced porosity, the area percentage μ has small variation at different welding velocities, and the lowest value can be obtained at the velocity of 2.0 m/min, the number of big porosity and total porosity area percentage also reach the lowest when the laser power is 5 kW and no defocusing value is adopted. For keeping the stability of keyhole, the heat input per unit time can be the highest at the lowest welding velocity, causing the increase of recoil pressure on the surface of keyhole, and then the unbalance of forces on keyhole and collapsing inside it occurs; more bubbles generate in molten pool. On the other hand, for escaping out from molten pool, it can be easier at a low welding velocity rate because the moving rate of solidification interface can be lower, too. The two factors affected the porosity remained in weld together, and 2.0 m/min is the most proper welding velocity to reduce the porosity in the weld at a laser power of 5 kW and a defocusing value of 0.

When the defocusing value of laser increases, it can be obviously found that the area percentage of both kinds of porosities and number of big porosity decrease, as shown in Figs. 3(e) and (f). The spot diameter of laser beam becomes larger with increasing the defocusing value, leading to lower energy density of laser beam on plate, thus the depth-to-width ratio of keyhole decreases. According to the liquid column model of KAWAGUCHI et al [7], the higher the depth-to-width ratio of keyhole is, the more unstable the keyhole is. On the other hand, the recoil pressure induced by evaporation of liquid fluid can be decreased when energy density is lower, which is positive to keep the keyhole stable during welding. So, the keyhole tends to be more unstable and the area percentage and number of porosity remained in weld get higher. It is deserved to point out that only two metallurgical pores with diameter of no more than 1.0 mm remained in weld at a defocusing value of +15 mm for no keyhole formed during the welding process, and both of them have a regular profile and smooth inner interface, so the assumption that porosity with regular feature can be identified to be metallurgical porosity is supported.

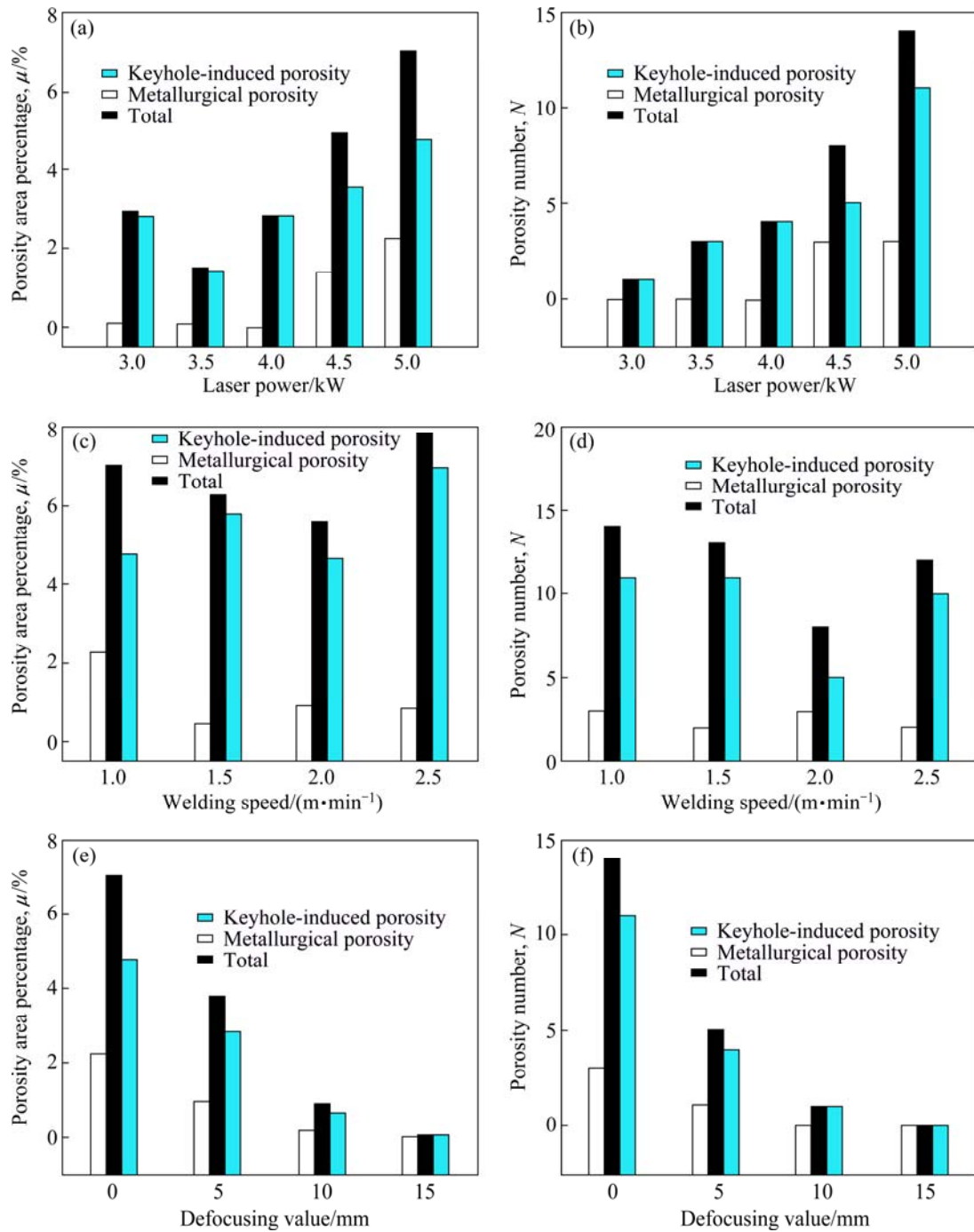


Fig. 3 Porosity area percentage and number of big porosity ($d > 1$ mm) at different process parameters: (a) Porosity area percentage at different laser powers; (b) Number of big porosity ($d > 1$ mm) at different laser power, $v_w = 1.0$ m/min, $D = 0$ mm; (c) Porosity percentage at different welding velocity; (d) Number of big porosity ($d > 1$ mm) at different welding velocities, $P = 5$ kW, $D = 0$ mm; (e) Porosity percentage area at different defocusing values; (f) Number of big porosity ($d > 1$ mm) at different defocusing values, $P = 5$ kW, $v_w = 1.0$ m/min

3.3 Variation of plume at different process parameters

The plume induced by ionized metallic vapor occurs over the keyhole in fiber laser welding process, and the violent variation of plume could reflect the intense evaporation inside the keyhole [20]. As shown in Fig. 4,

the shape and size of plasma are different at variant process parameters. Figure 4(a₁) shows the liquid metal spatter produced in welding process and Fig. 4(b₁) displays the profile of plume. The place of light point at the root of plume presents the location of the keyhole, shown in Fig. 4(d₁), brighter plume occurs at the opening

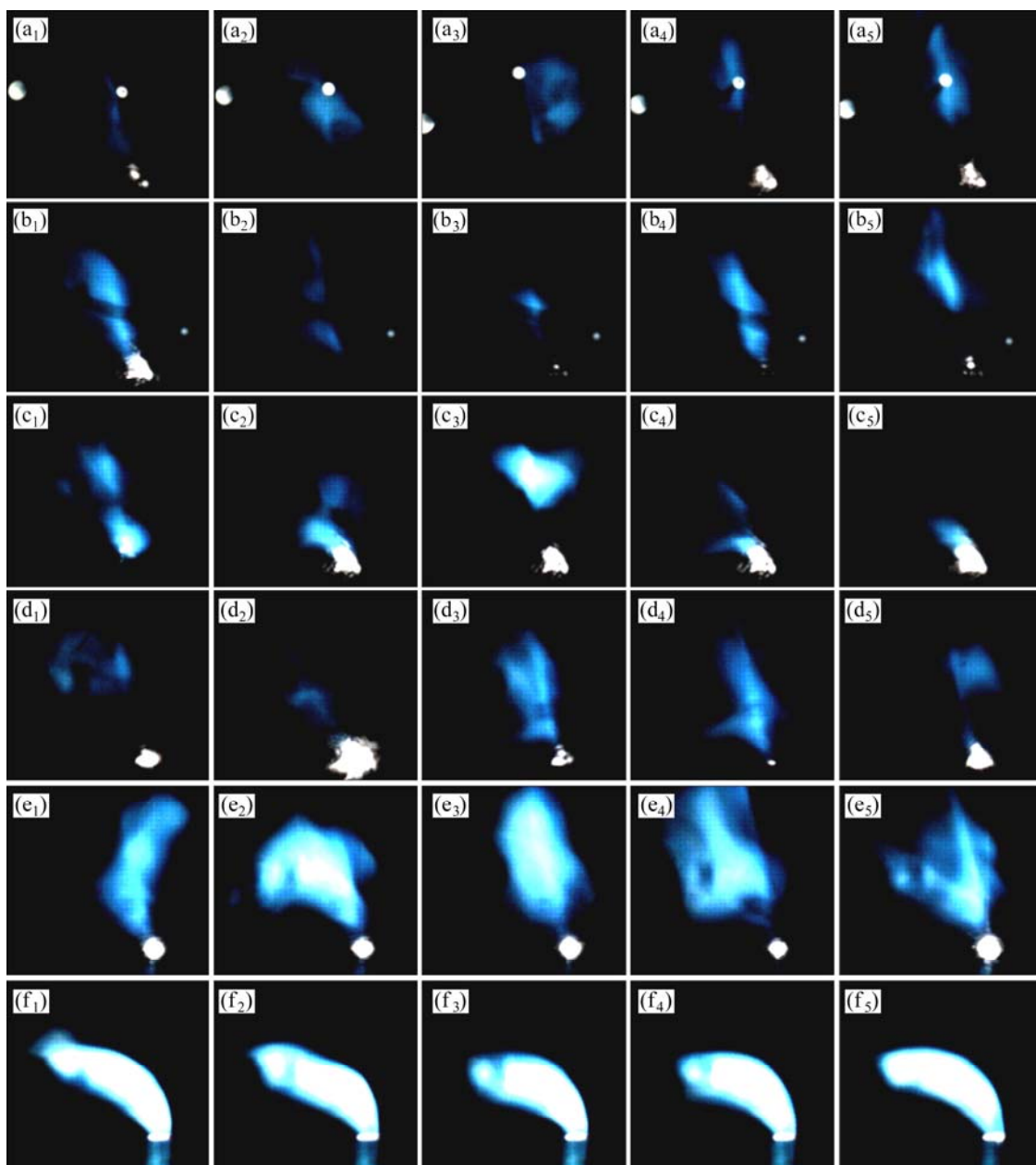


Fig. 4 Variation of plume at different process parameters during welding (1000 fps): (a₁–a₅) $P=5$ kW, $v_w=1.0$ m/min, $D=0$ mm; (b₁–b₅) $P=3$ kW, $v_w=1.0$ m/min, $D=0$ mm; (c₁–c₅) $P=5$ kW, $v_w=2.5$ m/min, $D=0$ mm; (d₁–d₅) $P=5$ kW, $v_w=1.0$ m/min, $D=+5$ mm; (e₁–e₅) $P=5$ kW, $v_w=1.0$ m/min, $D=+10$ mm; (f₁–f₅) $P=5$ kW, $v_w=1.0$ m/min, $D=+15$ mm (Time interval of one serious map 1 ms, (a₁) showing spatter induced in welding process, and (b₁) showing outline of plume, brightness of plasma affected by its density and reflection of laser beam from plate)

of keyhole because of the higher density of plume there.

Comparing the plume of Figs. 4(a₁–a₅) with (b₁–b₅), for higher laser power, the spatter induced by metallic vapor became more serious when the keyhole was exposed to higher laser power, and the shape and size of plume changed greatly at 5 kW power. The impact of metallic vapor in the keyhole tended to be stronger with increasing the heat input, leading to the unbalance of forces on keyhole, and more pores occurred on the weld at higher heat input due to unstable keyhole.

Figures 4(c₁–c₅) present less spatters in welding process when increasing welding velocity. The keyhole is more stable at higher welding velocity, there was no violent variation on the shape and size of plume, thus fewer bubbles (keyhole-induced) formed in welding process. However, as the welding velocity increased, the solidification rate increased simultaneously, leading to less time of bubbles growing, which caused the decrease of the number of large porosity. Affected by the two main factors, porosities in the weld appeared to be the

lowest at a welding speed of 2.0 m/min, as shown in Fig. 3(c).

The defocusing value affected the stability of keyhole obviously, as shown in Figs. 4(a₁–a₅), (d₁–d₅), (e₁–e₅) and (f₁–f₅). The variation of plume turned to be more stable as the defocusing value increased, less spatters appeared and the brightness of plume got higher. The spot size got larger as defocusing value grew, leading to lower penetration depth. The decrease of depth-to-width ratio helped to improve the stability of keyhole. The absorption of Al alloy to laser beam is extreme low without keyhole formation, for the laser may escape out of keyhole through multiple reflections [21]. So, the brightness of plume got higher since the reflected laser irradiated on it at larger defocusing value. At the same time, heat input in keyhole decreased as more laser escaped from keyhole. So, the impact of metallic vapor inside keyhole got weaker, the stability of keyhole kept good in welding process.

4 Conclusions

1) Metallurgical porosity is usually located at the middle of the weld, the microstructure is distributed uniformly and typical Al–Si dendrites with similar size can be found on the inside wall. Keyhole-induced porosity is often found at the root of the weld near the fusion line, the size and distribution of microstructure on the inner wall vary due to the complex temperature gradient caused by irregular shape of porosity.

2) The spatter and the violent variation of plume can reflect the instability inside the keyhole. More spatters occur when the recoil pressure and intense metallic vapor impact inside keyhole get stronger due to the extremely high energy density, and the variation of plume gets violent simultaneously.

3) Lower laser power or larger spot size can lead to fewer pores in the weld. Higher heat input can induce intense metallic vapor impact, thus causing the unbalance of forces on keyhole and collapse inside it. Also, larger spot size can lead to lower depth-to-width ratio of the keyhole which is positive to keep its stability, less bubbles appear and rarely pores remain in the weld. The porosity in the weld is determined by the combined action of stability of keyhole and moving rate of solidification interface at variant welding velocities. The total porosity area can reach the lowest at a welding speed of 2.0 m/min, when the laser power is 5 kW and defocusing value of 0 is adopted.

4) Increasing the defocusing value makes energy density low enough, at which no keyhole can be formed due to low recoil pressure. Only tiny metallurgical porosity occurs during the welding process, which can support the assumption that the pore with a regular shape

and smooth inner wall is metallurgical porosity.

Acknowledgments

The author would like to thank the technical support of Hui-ping WANG from General Motors Global Research and Development center of USA.

References

- [1] LEE J H, KIM J D, OH J S, PARK S J. Effect of Al coating conditions on laser weldability of Al coated steel sheet [J]. Transactions of Nonferrous Metals Society of China, 2009, 19(4): 946–951.
- [2] GAO Jin-qiang, QIN Guo-liang, YANG Jia-lin, HE Jian-guo, ZHANG Tao, WU Chuan-song. Image processing of weld pool and keyhole in Nd:YAG laser welding of stainless steel based on visual sensing [J]. Transactions of Nonferrous Metals Society of China, 2011, 21(2): 423–428.
- [3] YAO Wei, GONG Shui-li. Porosity formation mechanism and controlling technique for laser penetration welding [J]. Advanced Materials Research, 2011, 287: 2191–2194.
- [4] LIN R Y, HOCH M. The solubility of hydrogen in molten aluminum alloys [J]. Metallurgical Transactions A, 1989, 20(9): 1785–1791.
- [5] WANG Wei, XU Guang-ying, DUAN Ai-qin, WANG Xu-you, BA Rui-zhang. Formation mechanism of porosity in laser welding on 1420 Al–Li alloy [J]. Transactions of the China Welding Institution, 2005, 26(11): 59–62. (in Chinese)
- [6] KATAYAMA S, SETO N, MIZUTANI M, MATSUNAWA A. Formation mechanism of porosity in high power YAG laser welding [C]//Proceedings of the 3rd International Congress on Applications of Lasers and Electro-optics: ICALEO. Berlin: Springer–Verlag, 2000.
- [7] KAWAGUCHI I, TSUKAMOTO S, ARAKANE G, NAKATA K. Formation mechanism of porosity in deep penetration laser welding—Study on prevention of porosity in high power CO₂ laser welding (Report 2) [J]. Quarterly Journal of the Japan Welding Society, 2006, 24(4): 338–343.
- [8] SETO N, KATAYAMA S, MIZUTANI M, MATUNAWA A. Relationship between plasma and keyhole behavior during CO₂ laser welding [C]//Proceedings of Advanced High-power Lasers and Applications. Osaka: International Society for Optics and Photonics, 2000.
- [9] NORRIS J T, ROBINO C V, HIRSCHFELD D A, PERRICONE M J. Effects of laser parameters on porosity formation: Investigating millimeter scale continuous wave Nd:YAG laser welds [J]. Welding Journal, 2011, 90(10): 198–203.
- [10] MATSUNAWA A, MIZUTANI M, KATAYAMA S, SETO N. Porosity formation mechanism and its prevention in laser welding [J]. Welding International, 2003, 17(6): 431–437.
- [11] KUO T Y. Effects of pulsed and continuous Nd–YAG laser beam waves on welding of Inconel alloy [J]. Science and Technology of Welding & Joining, 2005, 10(5): 557–565.
- [12] KUO T Y, JENG S L. Porosity reduction in Nd–YAG laser welding of stainless steel and Inconel alloy by using a pulsed wave [J]. Journal of physics D: Applied Physics, 2005, 38(5): 722–728.
- [13] KATAYAMA S, UCHIUMI S, MIZUTANI M, WANG J, FUJII K. Penetration and porosity prevention mechanism in YAG laser–MIG hybrid welding [J]. Welding International, 2007, 21(1): 25–31.
- [14] ZHOU J, TSAI H L. Effects of electromagnetic force on melt flow and porosity prevention in pulsed laser keyhole welding [J]. International Journal of Heat and Mass Transfer, 2007, 50(11): 2217–2235.
- [15] ZHOU J, TSAI H L. Porosity formation and prevention in pulsed

- laser welding [J]. Journal of Heat Transfer, 2007, 129(8): 1014–1024.
- [16] ZHOU J, TSAI H L, WANG P C. Transport phenomena and keyhole dynamics during pulsed laser welding [J]. Journal of Heat Transfer, 2006, 128(7): 680–690.
- [17] CHO W I, NA S J, THOMY C, VOLLERTSEN F. Numerical simulation of molten pool dynamics in high power disk laser welding [J]. Journal of Materials Processing Technology, 2012, 212(1): 262–275.
- [18] ZHAO H Y, NIU W C, ZHANG B, LEI Y P, KODAMA M, ISHIDE T. Modelling of keyhole dynamics and porosity formation considering the adaptive keyhole shape and three-phase coupling during deep-penetration laser welding [J]. Journal of Physics D: Applied Physics, 2011, 44(48): 485302.
- [19] ZHOU J, TSAI H L, LEHNHOFF T F. Investigation of transport phenomena and defect formation in pulsed laser keyhole welding of zinc-coated steels [J]. Journal of Physics D: Applied Physics, 2006, 39(24): 5338–5355.
- [20] GAO X D, WEN Q, KATAYAMA S. Analysis of high-power disk laser welding stability based on classification of plume and spatter characteristics [J]. Transactions of Nonferrous Metals Society of China, 2013, 23(12): 3748–3757.
- [21] JIN Xiang-zhong. A three-dimensional model of multiple reflections for high-speed deep penetration laser welding based on an actual keyhole [J]. Optics and Lasers in Engineering, 2008, 46(1): 83–93.

光纤激光焊接 A356 铝合金过程气孔敏感性

李 凯^{1,2}, 芦凤桂^{1,2}, 郭松涛¹, 崔海超^{1,2}, 唐新华^{1,2}

1. 上海交通大学 材料科学与工程学院, 上海 200240;
2. 上海交通大学 上海市激光制造与材料改性重点实验室, 上海 200240

摘 要: 为减少激光深熔焊接铝合金过程中产生的冶金型气孔和小孔型气孔, 达到提高工件力学性能的目的, 系统分析激光功率、焊接速度以及离焦量等工艺参数分别对两种气孔造成的影响, 同时观察不同焊接参数下小孔上方的金属蒸汽羽烟形状与波动情况, 以反映焊接过程中小孔的稳定性。结果显示, 增加激光功率或减小激光光斑半径时, 小孔上方金属蒸汽羽烟波动剧烈, 形状和大小都极不稳定, 间接反映小孔的稳定性更差, 因此在焊缝根部产生更多小孔型气孔。当由激光能量密度变化引起的小孔深宽比增高时, 小孔内部坍塌的可能性升高, 并在焊缝中留下更多的气孔。当激光功率为 5 kW、离焦量为 0、焊接速度为 2.0 m/min 时, 气孔率达到最小值。

关键词: A356 铝合金; 光纤激光焊接; 气孔; 小孔; 蒸汽羽烟

(Edited by Wei-ping CHEN)